



Contents lists available at ScienceDirect

Catalysis Today

journal homepage: [www.elsevier.com/locate/cattod](http://www.elsevier.com/locate/cattod)

## New niobium heteropolyacid included in a silica/alumina matrix: Application in selective sulfoxidation

María B. Colombo Migliorero<sup>a,\*</sup>, Valeria Palermo<sup>a,\*</sup>, Gustavo P. Romanelli<sup>a,b</sup>, Patricia G. Vázquez<sup>a</sup>

<sup>a</sup> Centro de Investigación y Desarrollo en Ciencias Aplicadas "Dr. Jorge J. Ronco" CINDECA, (CONICET-CIC-UNLP), Facultad de Ciencias Exactas, Universidad Nacional de La Plata, Calle 47 N°257, B1900AJK, La Plata, Argentina

<sup>b</sup> Cátedra de Química Orgánica, Facultad de Ciencias Agrarias y Forestales, Universidad Nacional de La Plata, Calles 60 y 119 s/n, B1904AAN, La Plata, Argentina

### ARTICLE INFO

#### Keywords:

Silica/Alumina  
Niobium  
Heteropolyacid  
Sulfoxidation

### ABSTRACT

A new heteropolyacid, derived from phosphomolybdic acid containing niobium (PNbMo), was synthesized and included in silica, alumina, and silica/alumina matrixes by sol-gel technique, in order to use it as heterogeneous catalyst. The matrixes confer stability to the active phase, good textural and morphological properties. PNbMo and included materials were characterized by <sup>31</sup>P-NMR, FT-IR, UV-vis, TGA, SEM, TEM, XRD, N<sub>2</sub> physisorption, and potentiometric titration, and tested as catalyst in the sulfoxidation of diphenyl sulfide under suitable conditions. The redox activity was compared with phosphomolybdic acid and correlated with the edge energy obtained from UV-vis absorption spectra. The best results in diphenyl sulfide sulfoxidation were obtained with PNbMo-SiAl-4:1 (92% conversion and 95% selectivity at 3 h) and with PNbMo-Si (92% conversion and 94% selectivity at 4 h). The reuse of these catalysts was evaluated.

### 1. Introduction

Heteropolyacids (HPAs) are an important family of compounds largely used in catalysis [1–3]. They are composed of metal oxide clusters of early transition metals. The principal heteropolyanion is the Keggin structure (XM<sub>12</sub>O<sub>40</sub><sup>-</sup>), which consists of a central tetrahedron (XO<sub>4</sub>) encircled by twelve MO<sub>6</sub> that form M<sub>3</sub>O<sub>13</sub> (X = P<sup>5+</sup>, As<sup>5+</sup>, Si<sup>4+</sup>, and B<sup>3+</sup>; and M = W<sup>6+</sup> and Mo<sup>6+</sup>) [4]. One of the main Keggin heteropolyacids used as acid and redox catalyst is phosphomolybdic acid (H<sub>3</sub>PMo<sub>12</sub>O<sub>40</sub>, PMA), due to its strong acid strength and oxidation power. The substitution of one or more Mo atoms by V, which enhances the catalytic performance of HPA, has been widely reported in the literature [5–8]. Our research group has studied the catalytic capacity of PMA by substitution of one Mo atom by V, Bi, La, and Y [9–11]. The results encouraged us to employ other elements, in order to enhance the catalytic performance of PMA.

Niobium was chosen due its position in the periodic table: Nb belongs to the same period as Mo, and to V group. Besides, to our knowledge, there are no reports on Nb doped PMA in the literature. Nevertheless, some reports indicate the use of niobium in HPAs: for example, Nb<sub>2</sub>O<sub>5</sub> is used as support of HPA [12–15].

Park et al. [16] prepared H<sub>4</sub>PW<sub>11</sub>NbO<sub>40</sub> by hydrothermal treatment and evaluated its redox properties by electrochemical method and UV-vis absorption. Whereas, Zalomaeva et al. [17] reported on the use of Nb-monomo-substituted Lindqvist and Keggin polyoxotungstates as catalysts in the sulfide oxidation in acetonitrile, Maksimchuk et al. [18] used Nb-monomo-substituted Lindqvist polyoxotungstates in the epoxidation of alkenes, and Ren et al. [19] described a mixed Nb/W Dawson polyoxometalate.

Other niobium species used in catalysis are W-Nb-O and W-V-Nb-O mixed oxides, with hexagonal tungsten bronze structure, as catalysts in the one-pot oxidehydration of glycerol into acrylic acid [20]. Also, some niobium catalysts (NbCl<sub>5</sub>, Nb(OEt)<sub>5</sub>, mesoporous niobium silicate, Nb (Cp)<sub>2</sub>Cl<sub>2</sub> on silica) were used in sulfide [21] and alkene [22,23] oxidations with hydrogen peroxide.

Recently, Yang et al. [24] prepared multilayer-like polyoxometalates (HNbMoO<sub>6</sub>) by calcination of a stoichiometric mixture of Li<sub>2</sub>CO<sub>3</sub>, Nb<sub>2</sub>O<sub>5</sub>, and MoO<sub>3</sub> and subsequent acidification. This solid acid catalyst was used in the etherification of 5-hydroxymethylfurfural.

On the other hand, HPAs could be dissolved in various reaction media; for that reason many strategies to convert them to a heterogeneous catalyst have been developed by immobilization on a support

\* Corresponding authors.

E-mail addresses: [mbmigliorero@quimica.unlp.edu.ar](mailto:mbmigliorero@quimica.unlp.edu.ar) (M.B. Colombo Migliorero), [vpalermo@quimica.unlp.edu.ar](mailto:vpalermo@quimica.unlp.edu.ar) (V. Palermo).

<https://doi.org/10.1016/j.cattod.2020.10.034>

Received 26 March 2020; Received in revised form 12 August 2020; Accepted 21 October 2020

Available online 29 October 2020

0920-5861/© 2020 Elsevier B.V. All rights reserved.

[25], or by formation of an insoluble ionic material [4]. One strategy is to include the HPA in a solid matrix, such as silica, titania, and alumina [26,27], in order to turn it more stable and facilitate its isolation and recovery from the reaction media.

Sol-gel methodology allows the synthesis of micro and mesoporous materials with specific properties [28], for example, when HPAs are incorporated into a silica matrix, they provide stability to the Keggin structure and hinder the solubility in the reaction medium [9,29], and the alumina increases the catalytic activity [30].

Here, we describe the synthesis of phosphomolybdic acid doped with Nb, a new HPA derived from PMA, and included in silica, alumina, and two mixed silica/alumina frameworks, which confer stability to the active phase and good textural and morphological properties. The solid samples were characterized by several techniques (FT-IR, UV-vis, potentiometric titration, physisorption, among others).

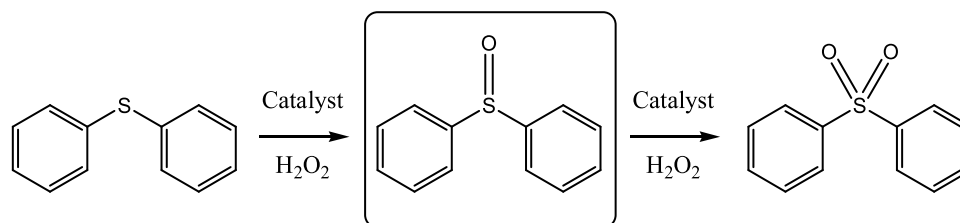
The new materials were examined as heterogeneous catalyst in a sulfoxidation reaction. This reaction was selected because many sulfides are important in the synthesis of biologically active molecules and natural products [31–33], asymmetric ligands [34], and oxygen transfer agents [35]. For sulfide oxidation, HPA acts together with aqueous hydrogen peroxide, instead of stoichiometric oxidants (nitric acids, trifluoroacetic acid) [36]. Selective oxidation of diphenyl sulfide (sulfoxidation) in an eco-friendly reaction condition, using aqueous hydrogen peroxide as oxidant and ethanol as solvent at 25 °C, was chosen as reaction test (Scheme 1).

## 2. Experimental

### 2.1. Catalyst synthesis

#### 2.1.1. General

Chemicals were acquired from Aldrich, Fluka and Merck, and used without further treatment. The reaction products were identified by comparative thin layer chromatography (TLC).



**Scheme 1.** Selective oxidation of diphenyl sulfide.

**Table 1**

HPA content, textural properties, and acid strength of samples.

Sample	HPA content (% w/w)	Specific surface area ( $S_{BET}$ ) (m <sup>2</sup> /gr)	Pore volume (cm <sup>3</sup> /gr)	Pore size (Å)	$E_0$ (mV)
PMA	100	19	0.02	4	822
PNbMo	100	7	0.01	7	768
SiO <sub>2</sub>	0	760	0.35	19	126
PMA-Si	15	702	0.30	20	377
PNbMo-Si	18	498	0.26	21	358
Al <sub>2</sub> O <sub>3</sub>	0	280	0.20	28	195
PMA-Al	14	339	0.32	37	86
PNbMo-Al	16	347	0.32	4	74
SiAl-1:1	0	299	0.76	101	295
PMA-SiAl-1:1	12	267	0.70	107	269
PNbMo-SiAl-1:1	16	303	0.45	59	185
SiAl-4:1	0	302	0.70	93	354
PMA-SiAl-4:1	10	289	0.50	73	377
PNbMo-SiAl-4:1	20	262	0.90	140	379

### 2.1.2. Heteropolyacid synthesis

PNbMo was synthesized by hydrothermal procedure [8] using a stoichiometric mixture of MoO<sub>3</sub> (110 mmol), Nb<sub>2</sub>O<sub>5</sub> (5 mmol), H<sub>3</sub>PO<sub>4</sub> 85% (w/v) (0.58 mL) suspended in distilled water (150 mL). The mixture was magnetically stirred for 6 h at 75 °C. Then, it was cooled to room temperature, and the insoluble materials were removed by filtration. The solution was evaporated at room temperature, and finally a dark green solid (PNbMo) was obtained.

### 2.1.3. Matrixes synthesis

Silica, alumina, and mixed SiAl-1:1 and SiAl-4:1 matrixes, were prepared according to reported methodology [37] (See Supplementary Material).

### 2.1.4. Synthesis of HPAs included in silica

PNbMo-Si (PNbMo included in silica) was prepared by mixing tetraethoxysilane (TEOS, 16 mmol) with absolute ethanol (80 mmol) under nitrogen atmosphere at room temperature. Then, under atmospheric conditions and stirring, a solution of PNbMo (0.75 g, 0.36 mmol) in absolute ethanol (36 mmol) and water (1.07 mL) were added, and continued stirring for 2 h to allow sol gelation. Finally, wet gel was aged until dry at room temperature.

For comparative purposes, PMA included in silica (PMA-Si) was synthesized in the same way as PNbMo-Si.

### 2.1.5. Synthesis of HPAs included in alumina

For PNbMo-Al (PNbMo included in alumina) synthesis, aluminum tri-sec-butoxide (TSBAL, 16 mmol) was mixed with absolute ethanol (174 mmol) under nitrogen atmosphere at room temperature. The mixture was retired from the controlled atmosphere and stirred until homogeneity. Then, hot distilled water (29.24 mL at 98 °C) was added and magnetically stirred at 90 °C. After 0.5 h, 0.75 g (0.36 mmol) of PNbMo was added and stirred 3 h at 90 °C. Finally, the gel was aged at 110 °C for 12 h.

For comparative purposes, we synthesized PMA included in alumina

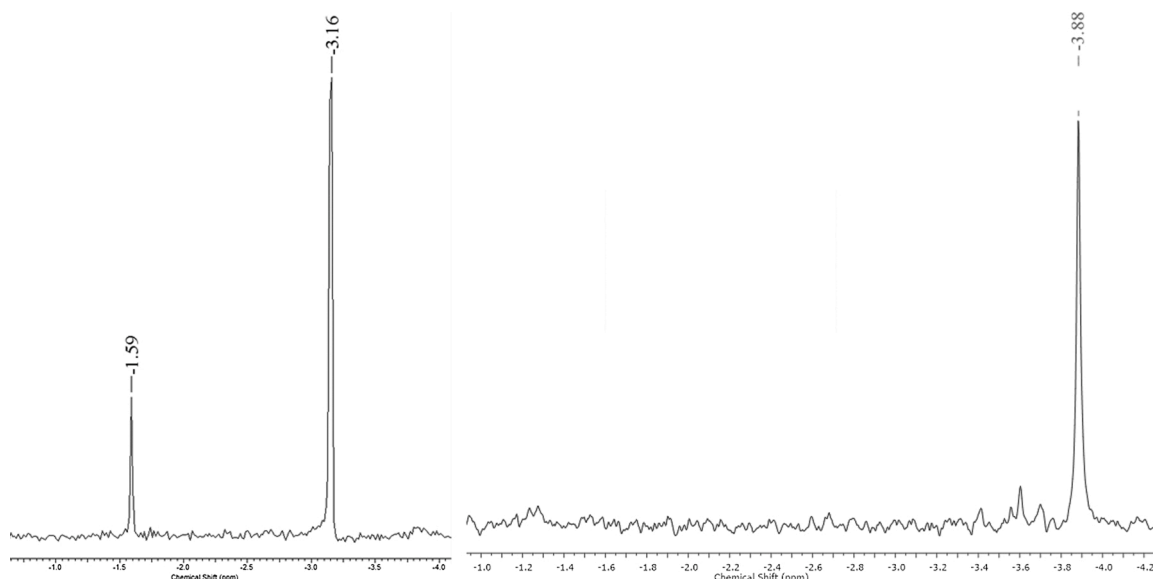


Fig. 1.  $^{31}\text{P}$ -NMR spectra of PNBMo (left) and PMA (right).

(PMA-Al) in the same way as PNBMo-Al.

#### 2.1.6. Synthesis of HPAs included in the mixed silica-alumina matrixes

PNbMo-SiAl-1:1 was prepared by mixing TEOS (8 mmol), TSBAI (8 mmol), and absolute ethanol (127 mmol) under nitrogen atmosphere at room temperature. The mixture was retired from the controlled atmosphere and stirred until homogeneity. Then, hot distilled water (15.15 mL at 98 °C) was added and magnetically stirred at 90 °C. After 0.5 h, 0.75 g (0.36 mmol) of PNBMo was added and stirred 3 h at 90 °C. Finally, the gel was aged at 110 °C for 12 h. For PNBMo-SiAl-4:1 synthesis, TEOS (13 mmol), TSBAI (3.25 mmol), and absolute ethanol (99 mmol) were mixed under nitrogen atmosphere. The mixture was retired from the controlled atmosphere and stirred until homogeneity. Then hot distilled water (6.70 mL at 98 °C) was added and magnetically stirred at 90 °C. After 0.5 h, 0.75 g (0.36 mmol) of PNBMo was added and stirred for 3 h. Finally, the gel was aged at 110 °C for 12 h.

For comparative purposes, we synthesized PMA included in PMA-SiAl-1:1 and PMA-SiAl-4:1 mixed oxides.

Finally, all solids were washed with ethanol and the final amount of HPA (Table 1) in the samples was calculated considering the final mass of the catalysts, the HPA mass used in the synthesis and not-incorporated HPA (remaining in the washing liquor).

## 2.2. Catalyst characterization

The  $^{31}\text{P}$ -NMR spectrum of PNBMo, in deuterated aqueous solution, was registered in Bruker Avance 300 equipment at a frequency of 121 MHz.

The UV-vis spectrum of solution of PNBMo in ethanol was measured with a Perkin Elmer Lambda 35 UV-vis double beam spectrophotometer, in the range 200–1100 nm at room temperature.

Thermogravimetric analysis (TGA) of bulk PNBMo was carried out with Shimadzu 50 equipment, in aluminum plate and air flow. The heating rate was 5 °C/min from 20 to 600 °C.

Fourier transform infrared spectra (FT-IR) were acquired using Bruker Vertex 70v equipment. The solid samples were ground and mixed with KBr, and pellets were formed. The measuring range was 400–4000  $\text{cm}^{-1}$ .

X-ray diffraction (XRD) patterns were recorded by means of a PANalytical X'Pert Pro 3373/00 device, using Cu K $\alpha$  radiation ( $\lambda = 1.5417 \text{ \AA}$ ), Ni filter, 20 mA and 40 kV in the high voltage source, scanning angle ( $2\theta$ ) from 5° to 40°, scanning rate 2° ( $2\theta$ )/min.

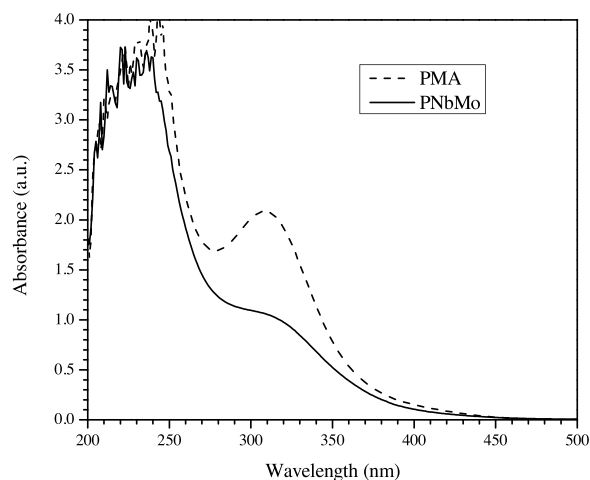


Fig. 2. UV-vis spectra of ethanolic solution of PNBMo and PMA.

Scanning electron microscopy (SEM) with energy dispersive X-ray spectroscopy (EDS) analysis was made with a Philips 505 scanning electron microscope using an accelerating voltage of 25 eV. The solid samples were metallized with Au. The chemical composition of the materials was analyzed by X-ray scattering.

PNbMo was also analyzed by transmission electron microscopy (TEM), in a JEOL 100 CX instrument, working at 100 kV. The sample was ultrasonically dispersed in ethanol and placed on a Formar® grid.

The total catalyst acidity was obtained by potentiometric titration by suspending the solid (0.025 g) in 45 mL of acetonitrile and titrating with a solution of *n*-butylamine in acetonitrile (0.025 N). The electrode potential (mV) variation was measured using the 794 Basic Titrino device with a Solvotrode electrode.

The specific surface area ( $S_{\text{BET}}$ ), pore volume, and the mean pore diameter of the included catalysts were determined by nitrogen adsorption/desorption. The samples were previously degasified for 700 min at 100 °C below 30 mm Hg, and the isotherms were obtained at -196 °C using Micromeritics ASAP 2020 equipment.

## 2.3. Catalytic activity

For the diphenyl sulfide oxidation test, catalysts (12 mg of bulk

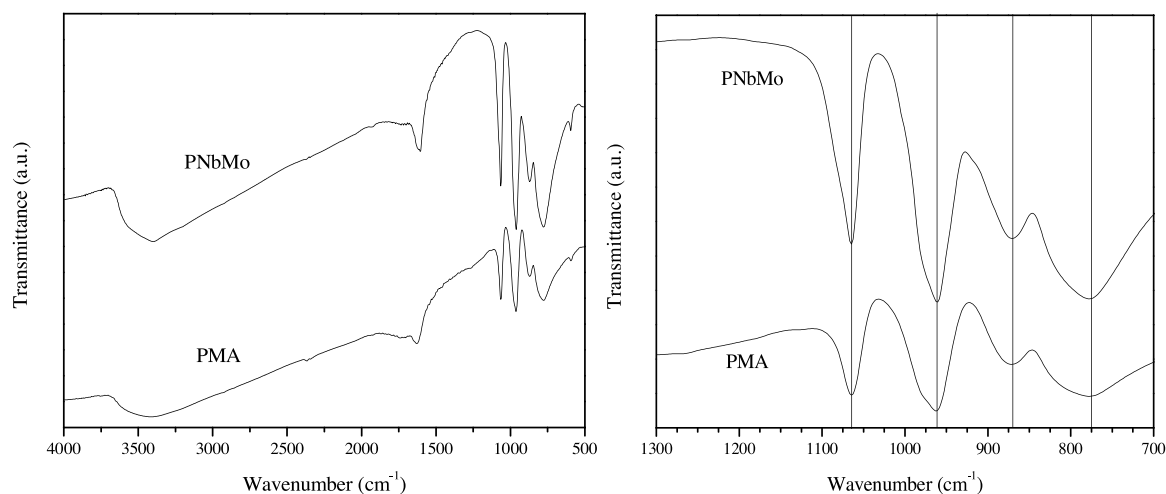


Fig. 3. FT-IR spectra of PNBMo and PMA.

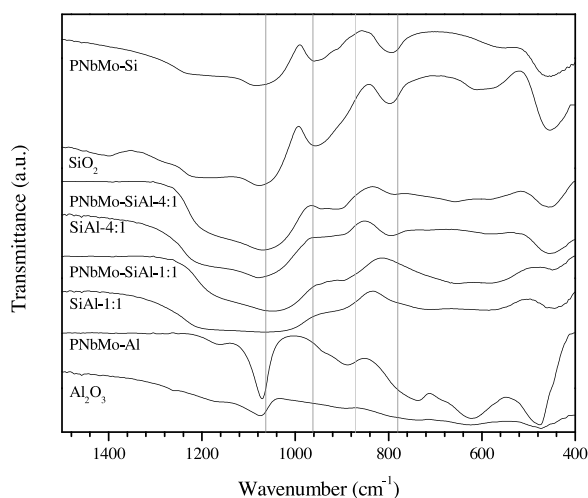


Fig. 4. FT-IR spectra of matrixes and included PNBMo.

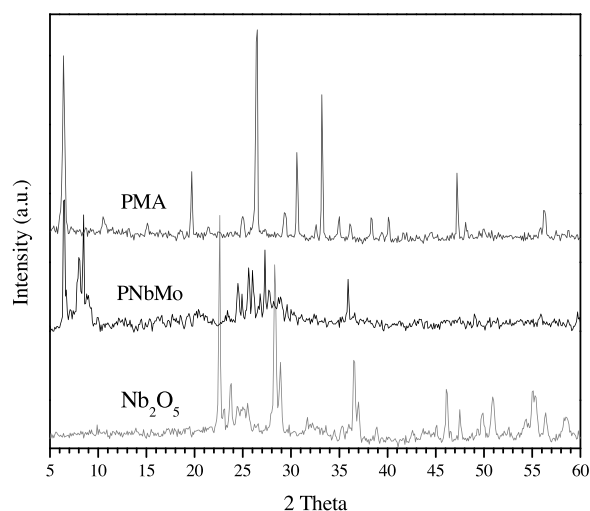


Fig. 5. XRD patterns of PNBMo, PMA, and Nb<sub>2</sub>O<sub>5</sub>.

PNbMo or PMA; 266 mg of included HPA), diphenyl sulfide (1 mmol), ethanol (8 mL), and aqueous H<sub>2</sub>O<sub>2</sub>, 35% (w/v) (1.5 mmol) were mixed in a glass reactor and stirred at 25 °C.

The reaction advance was examined by gas chromatography: samples of the reaction mixture (0.1 mL) were withdrawn after each hour, treated with dichloromethane (0.5 mL) and distilled water (0.5 mL). The organic layer was dried on anhydrous Na<sub>2</sub>SO<sub>4</sub>, filtered off, and analyzed by gas chromatography in a Shimadzu 2014 with a Supelco column (SPB-1, 30 m x 0.32 mm x 1 μm) and a flame ionization detector.

### 3. Results and discussion

#### 3.1. Characterization

The <sup>31</sup>P-NMR spectrum of PNBMo (Fig. 1) shows a major chemical shift at -3.16 ppm that can be associated with the Keggin unit of phosphomolybdate (the characteristic signal of PMA is at -3.88 ppm). It can be observed that the signal shifts to downfield by the presence of an atom different to Mo. The peak at -1.59 ppm can be assigned to lacunar species PMo<sub>11</sub> [38].

The UV-vis spectrum of PNBMo solutions is shown in Fig. 2. For comparative purposes, the spectrum of PMA is also included. The band assigned to oxygen-metal transfers at 210–260 nm can be seen in both spectra, and the band at 240–500 nm is assigned to octahedral Mo into

Keggin structure [39,40]. From these spectra it is possible calculate the absorption edge energy, which can be correlated with the redox properties of the HPA [41]. The edge energy for PNBMo is 3.22 eV, lower than the value calculated for PMA (3.36 eV), due to stabilization of the lowest unoccupied molecular orbital (LUMO) by the d-orbitals of niobium. A similar effect was observed by the replacement of molybdenum by vanadium in PMA [10].

The curve obtained by TGA (Supplementary Material, Fig. S1) shows that PNBMo has a weight loss of 12.6% between 20 °C and 200 °C, which corresponds to physisorbed water and allow calculating the hydration number of HPA (13 for PNBMo). From 200 °C to 450 °C, there is a small weight loss (1.45%) that corresponds to constitution water. The absence of major weight loss indicates that until 600 °C, the structure of HPA is thermally stable [42].

The FT-IR spectrum of PNBMo (Fig. 3) presents four bands at 1063 cm<sup>-1</sup>, 962 cm<sup>-1</sup>, 871 cm<sup>-1</sup>, and 780 cm<sup>-1</sup>, which are in agreement with the characteristic bands of Keggin structure PMA: 1064 cm<sup>-1</sup> (P-Oa), 962 cm<sup>-1</sup> (Mo = Od), 871 cm<sup>-1</sup> (Mo-Ob-Mo), 780 cm<sup>-1</sup> (Mo-Oc-Mo), where Oa connects the central tetrahedral P with Mo atoms, Ob links MoO<sub>6</sub> octahedra by the corners, Oc shares the octahedra edges, and Od are terminal atoms, bonded to one Mo atom [43]. This confirms that the synthesized PNBMo presents Keggin structure. A shoulder is observed for the P-Oa band, which could be assumed as a parameter of Mo-Oa interaction (a strong interaction corresponds to a weak stretching) [44].

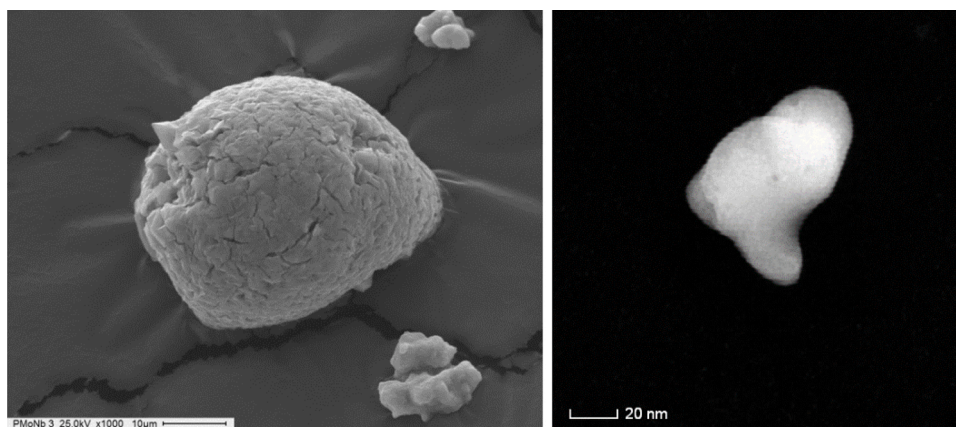


Fig. 6. SEM x1000 (left) and TEM (right) micrographs of PNBMo.

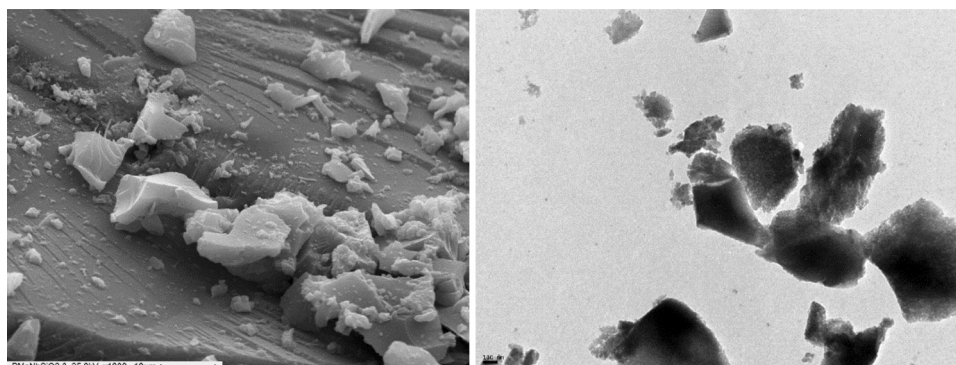


Fig. 7. SEM x1000 (left) and TEM (right) micrographs of PNBMo-Si.

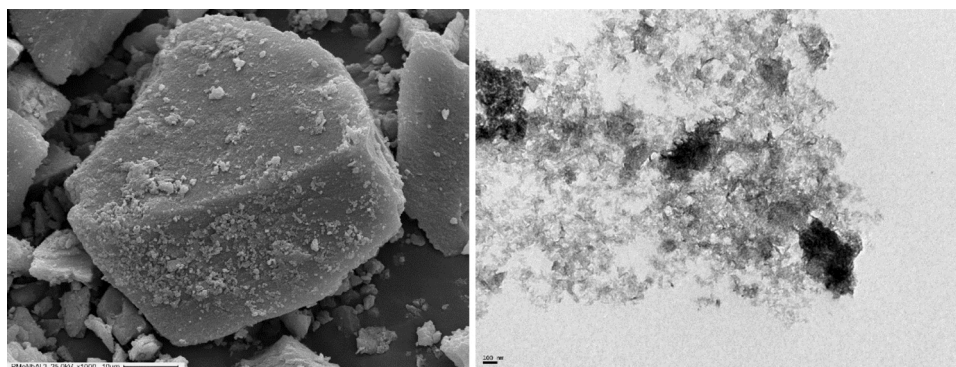


Fig. 8. SEM x1000 (left) and TEM (right) micrographs of PNBMo-Al.

Fig. 4 shows the  $1500\text{--}400\text{ cm}^{-1}$  region of the FT-IR spectra of matrixes and included PNBMo: PNBMo-Si, PNBMo-Al, PNBMo-SiAl-1:1, and PNBMo-SiAl-4:1. The characteristic signals of pure matrixes can be observed and the PNBMo bands (indicated by gray lines) are overlapped with those of the matrix.  $\text{Al}_2\text{O}_3$  has the characteristic bands of the boehmite structure:  $\nu\text{O-H}$   $3300\text{--}3500\text{ cm}^{-1}$ ,  $\delta\text{H}_2\text{O}$   $1635\text{ cm}^{-1}$ , and  $\delta\text{O-H}$   $1070\text{ cm}^{-1}$ . The band at  $620\text{ cm}^{-1}$  of  $\gamma$ -alumina [45,46] was not observed.  $\text{SiO}_2$  has the characteristic bands of the amorphous silica structure:  $\nu\text{O-Si-O}$   $1100\text{ cm}^{-1}$ ,  $\delta\text{O-Si-O}$   $800$  and  $1196\text{ cm}^{-1}$ ,  $\nu\text{Si-OH}$   $950\text{ cm}^{-1}$ ,  $\delta\text{Si-OH}$   $1640\text{ cm}^{-1}$ , and  $\delta\text{O-H}$   $3500\text{ cm}^{-1}$  [27]. In the spectra of the SiAl mixtures, the bands corresponding to both materials can be observed:  $3400$ ,  $1635$ ,  $1100$ , and  $800\text{ cm}^{-1}$ . (Full spectra are in Fig. S2 in Supplementary Material)

X-ray diffraction patterns of PNBMo and PMA are presented in Fig. 5.

The characteristic peaks of Keggin structure in the intervals  $6.5\text{--}10^\circ$ ,  $16.5\text{--}23^\circ$ , and  $25\text{--}36^\circ 2\theta$  are identified [47]. For comparison,  $\text{Nb}_2\text{O}_5$  pattern is included in the figure.

In X-ray diffraction patterns of included catalysts (Supplementary Material, Fig. S3) the PNBMo signals are masked by the matrixes patterns, which indicates a high dispersion. PNBMo-Si diffraction pattern is typical of an amorphous material, for PNBMo-Al the peaks appear at near  $15^\circ$ ,  $30^\circ$ ,  $40^\circ$ , and  $50^\circ 2\theta$ , corresponding to the boehmite structure [30,48]. PNBMo-SiAl-1:1 and PNBMo-SiAl-4:1 present the same shape of an amorphous material, because the broad bands of the silica masked the alumina and PNBMo signals.

The SEM and TEM images of PNBMo morphology are shown in Fig. 6. This HPA forms agglomerates of different sizes.

Figs. 7, 8, 9, 10 show the SEM and TEM micrographs of catalysts,

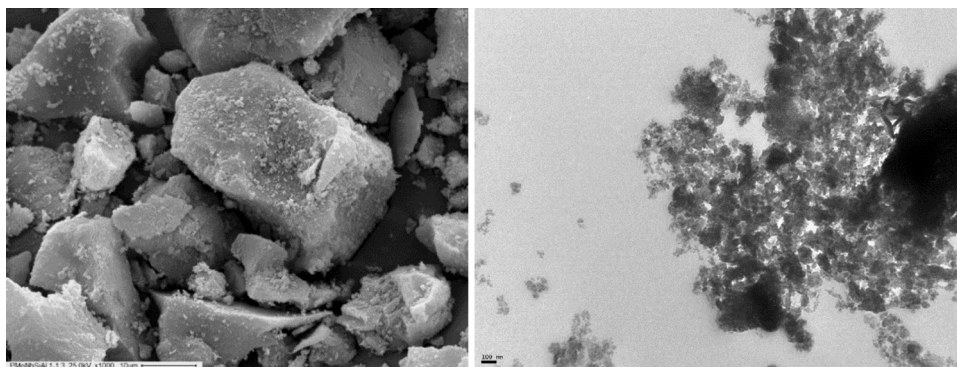


Fig. 9. SEM x1000 (left) and TEM (right) micrographs of PNBMo-SiAl-1:1.

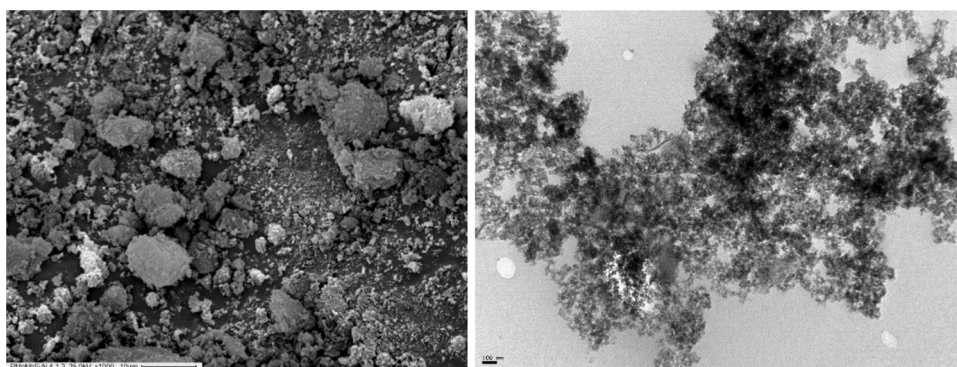


Fig. 10. SEM x1000 (left) and TEM (right) micrographs of PNBMo-SiAl-4:1.

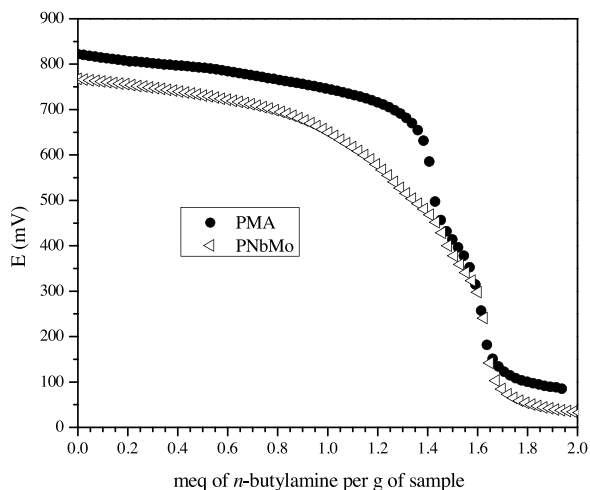


Fig. 11. Potentiometric titration with *n*-butylamine of PNBMo and PMA.

where laminar silica morphology and irregular morphology of alumina can be observed for PNBMo-Si and PNBMo-Al respectively [49]. For mixed silica-alumina materials, irregular morphology and size are appreciated in both catalysts. However, an increase in size is observed when the amount of Si is higher.

The total acidity of PNBMo was obtained by potentiometric titration with *n*-butylamine (Fig. 11). The maximum strength is indicated by the initial potential ( $E_0 = 768$  mV), and the total number of acid sites is given by the value of meq amine/g solid in the plateau. PNBMo has very strong acid sites, but a little lower than PMA ( $E_0 = 822$  mV).

The acid strength and the number of acid sites of PNBMo decrease when it is included in the matrixes (Table 1, Fig. 12). This could be

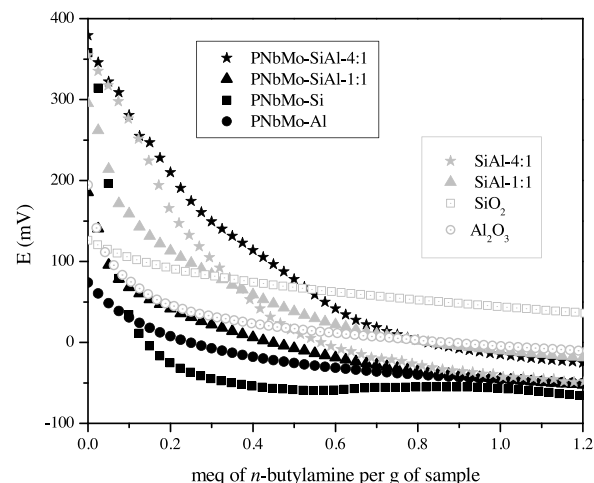


Fig. 12. Potentiometric titration with *n*-butylamine of included PNBMo and matrixes.

associated with the proton mobility of PNBMo within the framework. The curves are similar to those of the pure matrixes, and the same behavior was found for included PMA (Supplementary Material, Fig. S4). The acid strength of  $\text{SiO}_2$  and SiAl-4:1 increases when the HPA is included in them, but when the HPA is included in  $\text{Al}_2\text{O}_3$  or SiAl-1:1 matrix, the acid strength of the matrix decreases.

Nitrogen adsorption/desorption isotherms of mixed frameworks and HPAs included in them are shown in Figs. 13, 14. They present type II curves, characteristic of solids with large pores or nonporous [50]. Meanwhile, silica, PNBMo-Si, and PMA-Si are type I isotherms (Supplementary Material, Fig. S5), indicating a microporous material. A

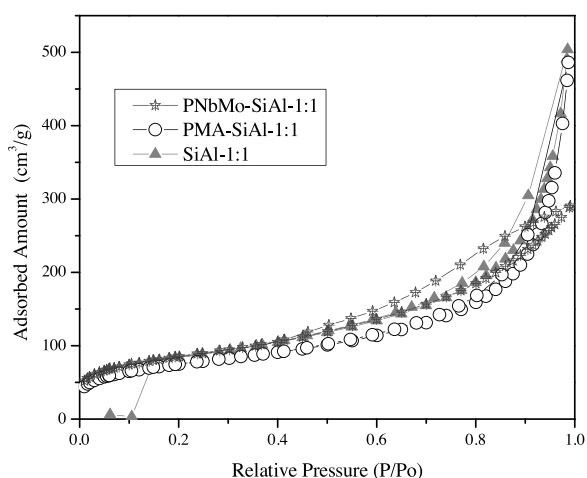


Fig. 13. Nitrogen adsorption/desorption isotherms of SiAl-1:1 and SiAl-1:1-included catalysts.

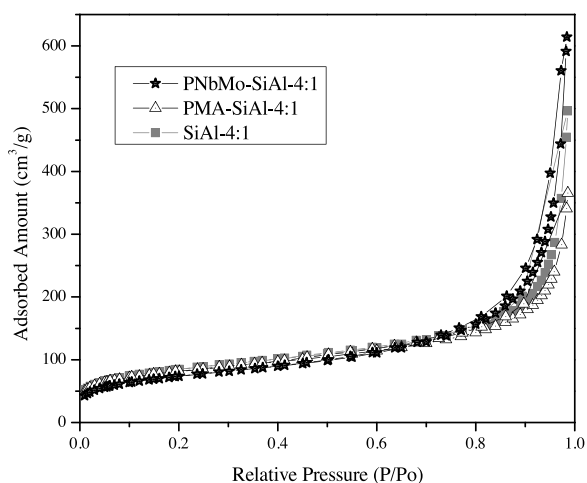


Fig. 14. Nitrogen adsorption/desorption isotherms of SiAl-4:1 and SiAl-4:1-included catalysts.

lower  $S_{BET}$  value than that of pure silica is probably due to pore blocking for the PNBMo inside the silica structure. On the other hand, pure alumina and HPA-Al present type IV isotherms (Supplementary

Material, Fig. S6), characteristic of mesoporous materials. The specific surface area ( $S_{BET}$ ) of matrixes and included PNBMo catalysts is listed in Table 1.

### 3.2. Catalytic activity

Diphenyl sulfide conversion (Scheme 1) was used to evaluate the catalytic performance of the new HPA doped with Nb. In a blank test, no conversion is observed when the reaction occurs in the absence of a catalyst, and only 15% conversion is reached with  $Nb_2O_5$  after 24 h of reaction (Fig. 15.a).

The incorporation of niobium in the Keggin structure results in a higher diphenyl sulfide conversion with respect to PMA. This agrees with the lower absorption edge energy calculated for PNBMo with respect to PMA obtained from UV-vis spectra, a result similar to that found when vanadium is incorporated in PMA structure [10].

The best results are obtained with PNBMo at 7 h (94% conversion and 94% diphenyl sulfoxide selectivity); at longer reaction times the selectivity to sulfoxide decreases (70% at 24 h), because it suffers the oxidation to diphenyl sulfone. Meanwhile, PMA produces only 36% of conversion at 7 h (100% diphenyl sulfoxide selectivity) but 98% of conversion and 94% of selectivity after 24 h (Table 2 and Fig. 15.a and b).

Then, the catalytic activity of included HPA was tested. The results show that the PNBMo catalysts produce higher values in diphenyl sulfide conversion than PMA catalysts (Table 2, Fig. 16.a). The matrixes without HPA inclusion were tested under the same reaction conditions. No conversion was observed using  $SiO_2$  after 24 h, but when  $Al_2O_3$  was used, 82% conversion and 65% selectivity were obtained. The mixed matrixes produced lower conversion and high selectivity (up to 95%) (Supplementary Material, Figure S7).

With respect to niobium-containing catalysts, high diphenyl sulfide conversion (near 100%) was reached after 5 h for all of them. However, at this time, the selectivity toward diphenyl sulfoxide was moderate (Table 2, Fig. 16.b) due to the subsequent oxidation of diphenyl sulfide to diphenyl sulfone. Taking into account the conversion and selectivity, the best results were obtained at 4 h with PNBMoSi (92% conversion and 94% selectivity), and at 3 h with PNBMo-SiAl-4:1 (92% conversion and 95% selectivity).

PNBMo-Si and PNBMo-SiAl-4:1 were selected to evaluate the reuse in the same reaction conditions. They were isolated from the reaction medium, washed with ethanol, dried under vacuum for the reuse. Taking into account the optimal reaction time for each catalyst, a slight decrease in the catalytic activity was achieved in the reuse of PNBMo-SiAl-4:1 at 3h: the conversion decreased from 92% to 82% in the

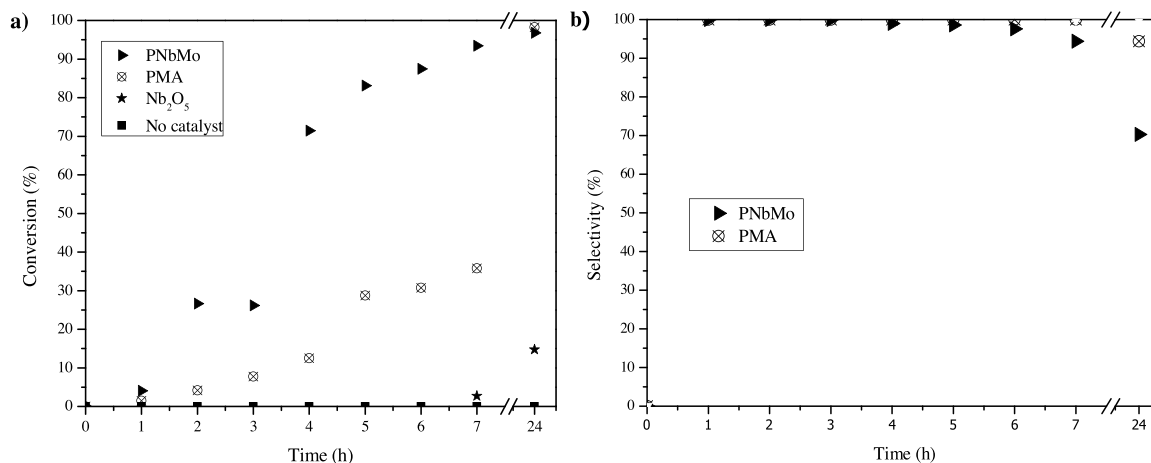
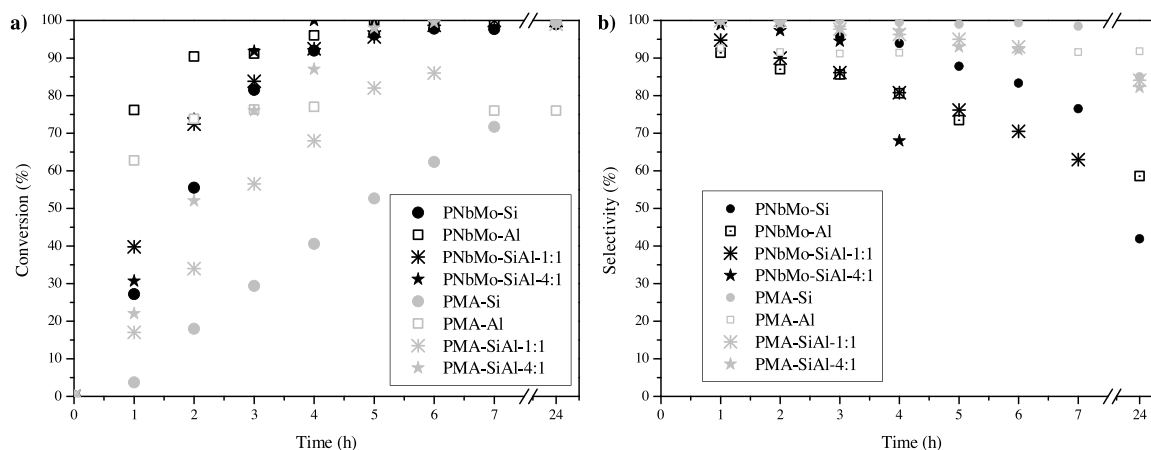


Fig. 15. Diphenyl sulfide conversion (a) and diphenyl sulfoxide selectivity (b) using bulk catalysts. Reaction conditions: catalyst (12 mg), diphenyl sulfide (1 mmol), ethanol (8 mL), and aqueous  $H_2O_2$ , 35% (w/v) (1.5 mmol), at 25 °C.

**Table 2**  
Diphenyl sulfide conversion and diphenyl sulfoxide selectivity obtained with the catalysts<sup>a</sup>.

Catalyst	Time (h)	Conv. (%)	Sel. (%)	Catalyst	Time (h)	Conv. (%)	Sel. (%)
PMA	1	2	100	PNbMo	1	4	100
	2	4	100		2	26	100
	3	8	100		3	26	100
	4	13	100		4	71	99
	5	29	100		5	83	99
	6	31	100		6	87	98
	7	36	100		7	94	94
	24	98	94	24	97	70	
PMA-Si	1	4	100	PNbMo-Si	1	27	100
	2	18	100		2	56	99
	3	29	100		3	81	96
	4	41	99		4	92	94
	5	53	99		5	96	88
	6	62	99		6	98	83
	7	72	98		7	98	76
	24	99	85	24	99	42	
PMA-Al	1	63	93	PNbMo-Al	1	76	91
	2	74	92		2	90	87
	3	76	91		3	91	86
	4	77	91		4	96	81
	24	76	92	24	100	59	
PMA-SiAl-1:1	1	17	100	PNbMo-SiAl-1:1	1	40	95
	2	34	100		2	72	90
	3	57	98		3	84	86
	4	68	96		4	93	81
	5	82	95		5	96	76
	6	86	93		6	99	71
	24	99	84	24	100	-	
PMA-SiAl-4:1	1	22	100	PNbMo-SiAl-4:1	1	31	99
	2	52	99		2	74	97
	3	76	95		3	92	95
	4	87	97		4	100	68
	5	98	93		5	100	-
	6	99	92		6	100	-
	24	100	82	24	100	-	

<sup>a</sup> Reaction conditions: catalyst (bulk: 12 mg or included: 266 mg), diphenyl sulfide (1 mmol), ethanol (8 mL), aqueous H<sub>2</sub>O<sub>2</sub>, 35% (w/v) (1.5 mmol) at 25 °C.



**Fig. 16.** Diphenyl sulfide conversion (a) and diphenyl sulfoxide selectivity (b) using included HPA. Reaction conditions: catalyst (266 mg), diphenyl sulfide (1 mmol), ethanol (8 mL), and aqueous H<sub>2</sub>O<sub>2</sub>, 35% (w/v) (1.5 mmol), at 25 °C.

reuse, and the selectivity toward diphenyl sulfoxide was 95% and 97%, in the first and second run, respectively. While, a bigger decrease was obtained with PNbMo-Si in the reuse after 4 h: the conversion dropped from 92% to 71%, and the selectivity was 94% and 99% in the use and reuse, respectively.

These results show that both matrixes are efficient for the inclusion PNbMo, allowing the use as recyclable catalyst in the selective sulfoxidation of diphenyl sulfide. Moreover, mixed framework SiAl-4:1,

present better performance in the reuse.

#### 4. Conclusions

A heteropolyacid (PNbMo) derived from PMA doped with niobium was synthesized by hydrothermal method. The Keggin structure was confirmed by FT-IR, XRD, and <sup>31</sup>P-NMR characterization. The catalytic activity was tested in the diphenyl sulfide sulfoxidation, compared with

PMA and correlated with the absorption edge energy calculated from UV-vis spectra.

The heteropolyacids were included in silica, alumina, and mixed silica/alumina matrixes by sol-gel technique, in order to convert PNBMo to a heterogeneous catalyst. The solids were widely characterized, and the catalytic performance was tested. Silica and mixed frameworks conferred stability, hindered the solubility, and provided good textural and morphological properties. The redox property of the heteropolyacid was maintained when it was included in a matrix, and good results were achieved in the diphenyl sulfide sulfoxidation using aqueous H<sub>2</sub>O<sub>2</sub>, under mild reaction conditions. The best results were obtained with PNBMo-SiAl-4:1 (92% conversion and 95% selectivity at 3 h) and with PNBMo-Si (92% conversion and 94% selectivity at 4 h). The reuse of the catalysts with best performance was evaluated, and only a slight decrease in the conversion was detected. These catalysts are promising for the sulfoxidation of more complex sulfides.

### CRediT authorship contribution statement

**María B. Colombo Migliorero:** Methodology, Investigation, Data curation, Formal analysis, Writing - review & editing. **Valeria Palermo:** Methodology, Supervision, Investigation, Formal analysis, Writing - original draft, Writing - review & editing. **Gustavo P. Romanelli:** Conceptualization, Methodology, Supervision, Formal analysis, Writing - review & editing, Funding acquisition, Project administration. **Patricia G. Vázquez:** Conceptualization, Methodology, Supervision, Formal analysis, Writing - review & editing, Funding acquisition.

### Declaration of Competing Interest

The authors declare that they have no known competing financial interests or personal relationships that could have appeared to influence the work reported in this paper.

### Acknowledgments

The authors thank L. Osiglio, J. Tara, M. Theiller, I.D. Lick, G. Kürten, M.J. Yañez, and A. Caneiro for the experimental measurements. We also thank UNLP (X774), CONICET (PIP0321), and ANPCyT (PICT 2013-0409; PICT 2017-2174) for the financial support.

### Appendix A. Supplementary data

Supplementary material related to this article can be found, in the online version, at doi:<https://doi.org/10.1016/j.cattod.2020.10.034>.

### References

- [1] L.M. Sanchez, H.J. Thomas, M.J. Climent, G.P. Romanelli, S. Iborra, *Catal. Rev.* 58 (2016) 497–586.
- [2] M. Misono, *Catalysis of heteropoly compounds (Polyoxometalates)*, *Stud. Surf. Sci. Catal.* 176 (2013) 97–155.
- [3] S.-S. Wang, G.-Y. Yang, *Chem. Rev.* 115 (2015) 4893–4962.
- [4] N. Mizuno, K. Kamata, S. Uchida, K. Yamaguchi, *Liquid-phase oxidations with hydrogen peroxide and molecular oxygen catalyzed by polyoxometalate-based compounds*, in: N. Mizuno (Ed.), *Modern Heterogeneous Oxidation Catalysis Design, Reactions and Characterization*, WILEY-VCH, Weinheim, 2009, pp. 185–216.
- [5] T. Okuhara, N. Mizuno, M. Misono, *Adv. Catal.* 41 (1996) 113–252.
- [6] I.V. Kozhevnikov, *Chem. Rev.* 98 (1998) 171–198.
- [7] M.M. Heravi, S. Sadjadi, *J. Iran. Chem. Soc.* 6 (2009) 1–54.
- [8] P. Villabril, G. Romanelli, P. Vázquez, C. Cáceres, *Appl. Catal. A Gen.* 270 (2004) 101–111.

- [9] V. Palermo, G.P. Romanelli, P.G. Vázquez, *J. Mol. Catal. A Chem.* 373 (2013) 142–150.
- [10] V. Palermo, Á.G. Sathicq, P.G. Vázquez, H.J. Thomas, G.P. Romanelli, *React. Kinet. Mech. Catal.* 104 (2011) 181–195.
- [11] O. D'alessandro, Á. Sathicq, V. Palermo, L. Sanchez, H. Thomas, P. Vazquez, T. Constantieux, G. Romanelli, *Curr. Org. Chem.* 16 (2012) 2763–2769.
- [12] M. Ziolk, *Catal. Today* 78 (2003) 47–64.
- [13] E. Caliman, J.A. Dias, S.C.L. Dias, F.A.C. Garcia, J.L. De Macedo, L.S. Almeida, *Microporous Mesoporous Mater.* 132 (2010) 103–111.
- [14] L.R.V. da Conceição, L.M. Carneiro, D.S. Giordani, H.F. de Castro, *Renew. Energy* 113 (2017) 119–128.
- [15] S. An, D. Song, Y. Sun, Y. Guo, Q. Shang, *Microporous Mesoporous Mater.* 226 (2016) 396–405.
- [16] D.R. Park, S.H. Song, U.G. Hong, J.G. Seo, J.C. Jung, I.K. Song, *Catal. Lett.* 132 (2009) 363–369.
- [17] O.V. Zalomaeva, N.V. Maksimchuk, G.M. Maksimov, O.A. Kholdeeva, *Eur. J. Inorg. Chem.* 2 (2019) 66–68.
- [18] N.V. Maksimchuk, G.M. Maksimov, V.Y. Evtushok, I.D. Ivanchikova, Y.A. Chesalov, R.I. Maksimovskaya, O.A. Kholdeeva, A. Solé-Daura, J.M. Poblet, J.J. Carbó, *ACS Catal.* 8 (2018) 9722–9737.
- [19] Y. Ren, Y. Hu, Y. Shan, Z. Kong, M. Gu, B. Yue, H. He, *Inorg. Chem. Commun.* 40 (2014) 108–111.
- [20] A. Chierigato, F. Basile, P. Concepción, S. Guidetti, G. Liosi, M. Dolores, C. Trevisan, F. Cavani, J.M. López, *Catal. Today* 197 (2012) 58–65.
- [21] M. Kirihara, J. Yamamoto, T. Noguchi, A. Itou, S. Naito, Y. Hirai, *Tetrahedron* 65 (2009) 10477–10484.
- [22] I.D. Ivanchikova, N.V. Maksimchuk, I.Y. Skobelev, V.V. Kaichev, O.A. Kholdeeva, *J. Catal.* 332 (2015) 138–148.
- [23] S. Dworakowska, C. Tiozzo, M. Niemczyk-Wrzeszcz, P. Michorczyk, N. Ravasio, R. Psaro, D. Bogda, M. Guidotti, *J. Clean. Prod.* 166 (2017) 901–909.
- [24] F. Yang, J. Tang, R. Ou, Z. Guo, S. Gao, Y. Wang, X. Wang, *Appl. Catal. B Environ.* 256 (2019), 117786.
- [25] E.F. Freitas, M.F. Paiva, S.C.L. Dias, J.A. Dias, *Catal. Today* 289 (2017) 70–77.
- [26] G. Pasquale, P. Vázquez, G. Romanelli, G. Baronetti, *Catal. Commun.* 18 (2012) 115–120.
- [27] V. Palermo, Á. Sathicq, T. Constantieux, J. Rodríguez, P. Vázquez, G. Romanelli, *Catal. Letters* 145 (2015) 1022–1032.
- [28] S. Soltani, U. Rashid, S.I. Al-Resayes, I.A. Nehdi, *Energy Convers. Manage.* 141 (2017) 183–205.
- [29] G. Romanelli, P. Vázquez, L. Pizzio, N. Quaranta, J. Autino, M. Blanco, C. Cáceres, *Appl. Catal. A Gen.* 261 (2004) 163–170.
- [30] S. Thanasilp, J.W. Schwank, V. Meeyoo, *J. Mol. Catal. A Chem.* 380 (2013) 49–56.
- [31] E.N. Prilezhaeva, *Russ. Chem. Rev.* 70 (2001) 897–920.
- [32] A. Kalir, H.H. Kalir, *Biological activity of sulfoxides and sulfones*, in: S. Patai, Z. Rappoport (Eds.), *The Chemistry of Sulphur-Containing Functional Groups*, Wiley, New York, 1993, pp. 957–973.
- [33] J. Legros, J.R. Dehli, C. Bolm, *Adv. Synth. Catal.* 347 (2005) 19–31.
- [34] I. Fernández, N. Khair, *Chem. Rev.* 103 (2003) 3651–3705.
- [35] V.Y. Kukushkin, *Coord. Chem. Rev.* 139 (1995) 375–407.
- [36] F. Liu, Z. Fu, Y. Liu, C. Lu, Y. Wu, F. Xie, Z. Ye, X. Zhou, D. Yin, *Ind. Eng. Chem. Res.* 49 (2010) 2533–2536.
- [37] M.B. Colombo Migliorero, V. Palermo, G.P. Romanelli, P.G. Vázquez, *An. Asoc. Quim.* 106 (2019) 47–55.
- [38] A.B. Vishnikin, T.Y. Svinarenko, H. Sklenářová, P. Solich, Y.R. Bazel, V. Andrich, *Talanta* 80 (2010) 1838–1845.
- [39] P. Mothé-Esteves, M. Maciel Pereira, J. Arichi, B. Louis, *Cryst. Growth Des.* 10 (2010) 371–378.
- [40] R. de Paiva Floro Bonfim, L.C. de Moura, H. Pizzala, S. Caldarelli, S. Paul, J.G. Eon, O. Mentre, M. Capron, L. Delevoe, E. Payen, *Inorg. Chem.* 46 (2007) 7371–7377.
- [41] K.P. Barteau, J.E. Lyons, I.K. Song, M.A. Barteau, *Top. Catal.* 41 (2006) 55–62.
- [42] V. Sasca, M. Ștefănescu, A. Popa, *J. Therm. Anal. Calorim.* 56 (1999) 569–578.
- [43] L.R. Pizzio, P.G. Vázquez, C.V. Cáceres, M.N. Blanco, *Appl. Catal. A Gen.* 256 (2003) 125–139.
- [44] C. Rocchiccioli-Deltcheff, A. Aouissi, M.M. Bettahar, S. Launay, M. Fournier, *J. Catal.* 164 (1996) 16–27.
- [45] M. Jafar Tafreshi, Z. Masoomi Khanghah, *Mater. Sci.* 21 (2015) 28–31.
- [46] S. Musić, D. Dragčević, S. Popović, *Mater. Lett.* 40 (1999) 269–274.
- [47] A. Popa, V. Sasca, E.E. Kiss, R. Marinkovic-Neducin, M.T. Bokorov, I. Holclajtner-Antunović, *Mater. Chem. Phys.* 119 (2010) 465–470.
- [48] D.N. Zambrano, M.O. Gosatti, L.M. Dufou, D.A. Serrano, M.M. Guraya, S. Perez-Catán, *Int. J. Min. Met. Mater.* 10 (2016) 598–603.
- [49] M. Wannaborworn, P. Praserttham, B. Jongsomjit, *J. Nanomater.* 2015 (2015), 519425.
- [50] J.D. Wright, N.A.J.M. Sommerdijk, *Sol-Gel Materials Chemistry and Applications*, Taylor & Francis Group, Boca Raton, 2001.